Altered expression of mir-222 and mir-25 influences diverse gene expression changes in transformed normal and anaplastic thyroid cells, and impacts on MEK and TRAIL protein expression

SINÉAD T. AHERNE[1], PAUL SMYTH[2], MICHAEL FREELEY[3], LEILA SMITH[4], CATHY SPILLANE[2], JOHN O'LEARY[2] and ORLA SHEILS[2]

[1]National Institute for Cellular Biotechnology, Dublin City University, Glasnevin, Dublin 9; [2]Department of Histopathology; [3]Department of Clinical Medicine and Trinity Translational Medicine Institute, Trinity College Dublin, Dublin 8, Republic of Ireland; [4]Fluidigm Corporation, Suite 100, South San Francisco, CA 94080, USA

Received January 9, 2016; Accepted March 21, 2016

DOI: 10.3892/ijmm.2016.2653

Abstract. Thyroid cancer is the most common endocrine malignancy and accounts for the majority of endocrine cancer-related deaths each year. Our group and others have previously demonstrated dysfunctional microRNA (miRNA or miR) expression in the context of thyroid cancer. The objective of the present study was to investigate the impact of synthetic manipulation of expression of miR-25 and miR-222 in benign and malignant thyroid cells. miR-25 and miR-222 expression was upregulated in 8505C (an anaplastic thyroid cell line) and Nthy-ori (a SV40-immortalised thyroid cell line) cells, respectively. A transcriptomics-based approach was utilised to identify targets of the two miRNAs and real-time PCR and western blotting were used to validate a subset of the targets. Almost 100 mRNAs of diverse functions were found to be either directly or indirectly targeted by both miR-222 and miR-25 [fold change ≥2, false discovery rate (FDR) ≤0.05]. Gene ontology analysis showed the miR-25 gene target list to be significantly enriched for genes involved in cell adhesion. Fluidigm real-time PCR technologies were used to validate the downregulation of 23 and 22 genes in response to miR-25 and miR-222 overexpression, respectively. The reduction of the expression of two miR-25 protein targets, TNF-related apoptosis-inducing ligand (TRAIL) and mitogen-activated protein kinase kinase 4 (MEK4), was also validated. Manipulating the expression of both miR-222 and miR-25 influenced diverse gene expression changes in thyroid cells. Increased expression of miR-25 reduced MEK4 and TRAIL protein expression, and cell adhesion and apoptosis are important aspects of miR-25 functioning in thyroid cells.

Correspondence to: Dr Sinéad T. Aherne, National Institute for Cellular Biotechnology, Dublin City University, Collins Avenue, Glasnevin, Dublin 9, Republic of Ireland
E-mail: sinead.aherne@dcu.ie

Abbreviations: MAPK, mitogen-activated protein kinase; hTERT, human telomerase reverse transcriptase; FDR, false discovery rate; RIPA, radioimmunoprecipitation assay; DR4, TRAIL death receptor-4; PSG, pregnancy-specific glycoprotein; TRAIL, TNF-related apoptosis-inducing ligand; IKK complex, inhibitor of κB kinase complex; ERK, extracellular regulated kinases; JNK, c-Jun NH2-terminal kinase

Key words: thyroid cancer, miR-222 and miR-25, microarray, target genes, mitogen-activated protein kinase kinase 4 and TNF-related apoptosis-inducing ligand

Introduction

Thyroid cancer is the most common endocrine malignancy, and incidences are on the rise worldwide. Thyroid tumours frequently possess genetic alterations which lead to the activation of the mitogen-activated protein kinase (MAPK) signalling pathway (1). The expression of microRNAs (miRNAs or miRs) has been studied in thyroid cancers, and as with other types of cancer, miRNA profiles have been found to be significantly different between tumours of the thyroid compared to normal thyroid tissue. For instance miR-146, miR-221, miR-222, miR-155, miR-181a and miR-181b have been shown to differentiate papillary thyroid cancer from normal thyroid tissue (2,3).

miRNAs have also shown differential expression between different types of thyroid cancer (4) and within a multifocal pluriform tumour from an individual thyroid gland (5), thus illustrating that miRNA profiles have demonstrated both intra- and inter-tumour variability. The functions of some of these differentially expressed miRNAs have also been elucidated: for instance, miR-221 has been shown to regulate *HOXB5* (6) and the human telomerase reverse transcriptase (*hTERT*) gene is regulated by miR-138 (7). Furthermore, the potential utility of these small molecules to aid thyroid cancer diagnosis (8) and prognosis (9) has also been investigated.

The aim of the present study was to elucidate the target mRNAs of two miRNAs that we had previously found to be differentially expressed in thyroid cancer (5): miR-222 and miR-25. miR-222 is commonly found to be upregulated in thyroid cancer (2-4) and is part of an intergenic miRNA cluster (that also contains miR-221) on the p11.3 region of the X chromosome. It is one of the most well-known miRNAs linked to

thyroid cancer, and some of its gene targets have been elucidated, including the *KIT* gene (2) and the $p27^{Kip1}$ protein (10).

miR-25 is also located in a miRNA cluster, termed the mi-106b-25 cluster. miR-106b and miR-93 are the two other miRNAs in this highly conserved cluster which is located in a 515-bp region at chromosome 7q22, in intron 13 of the host gene *MCM7*. The miRNAs are co-transcribed in the context of the *MCM7* primary transcript and have been found to accumulate in different types of cancer, including gastric, prostate, pancreatic neuroendocrine tumours, neuroblastoma and multiple myeloma (11). miR-25 has been shown to regulate p57 (12) and E2F1 as part of a negative feedback loop in gastric cancer (11). It has also been shown to promote cell invasion and migration in esophageal squamous cell carcinoma (13) and regulate apoptosis by targeting the Bim protein in ovarian (14) and eosophangeal cells (15). miR-25 has been found to be downregulated in anaplastic thyroid carcinoma (16) and, along with miR-30d, to target the polycomb protein enhancer of zeste 2 (EZH2) in this disease context (17).

In this study, we describe work in which we examined the impact of upregulating the thyroid cancer-associated miRNA miR-222 in benign Nthy-ori cells, and miR-25, a miRNA downregulated in anaplastic thyroid cancer, in the anaplastic cancer-derived 8505C cell line. Microarray technologies were utilised to monitor global gene expression changes in response to altered expression of miR-222 and miR-25. This unbiased genome-wide approach provided by the microarrays yielded the discovery of almost 100 mRNAs that are either directly or indirectly targeted by each miRNA in thyroid cells and have not been previously described to the best of our knowledge. These gene lists provide insights as to the functions of these miRNAs within thyroid cells; they contain both predicted and novel targets of the miRNAs, a subset of which were validated at the mRNA and protein level.

Materials and methods

Cell culture. The human thyroid follicular epithelial cell line Nthy-ori 3-1 (cat no. 90011609; ECACC, Salisbury, UK) was grown in RPMI media containing 10% foetal bovine serum (FBS), 2% penicillin/streptomycin (5,000 U/ml). An undifferentiated human thyroid carcinoma cell line, 8505C, (cat no. 94090184; ECACC) was grown in Eagle's minimum essential medium (EMEM) with Hank's buffered salt solution (HBSS) containing 2 mM glutamine and 1% non-essential amino acids (NEAA), 10% FBS, and 2% penicillin/streptomycin (5,000 U/ml). All cell culture reagents were purchased from Lonza (Basel, Switzerland) and cells were incubated at 37˚C in a 5% CO_2 humidified chamber (series II water jacketed CO_2 incubator; Thermo Fisher Scientific, Waltham, MA, USA).

Transfections. For transfections, Nthy-ori 3-1 and 8505C cells were plated at a density of $1.5x10^5$ cells/ml in 12-well plates (Nalge Nunc, Penfield, NY, USA) with three replicate wells for each condition. Cells were reverse transfected using Lipofectamine 2000 (Invitrogen, Grand Island, NY, USA) according to the manufacturer's instructions with 50 nM pre-miR positive control (cat. # AM17150), pre-miR negative control #1 (cat. # AM17110), pre-miR-222 (cat. # PM11376) or pre-miR-25 (cat. # PM12401) (Ambion, Austin, TX, USA).

Transfection efficiency was evaluated using TaqMan real-time polymerase chain reaction (PCR) as follows. Pre-miR hsa-miR-1 miRNA precursor was used as a positive control in transfection experiments as, upon delivery into cells, it effectively downregulates the expression of *PTK9* at the mRNA level. Effective delivery and activity of the pre-miR hsa-miR-1 miRNA precursor was detected by real-time PCR using a TaqMan Gene Expression assay to PTK9 (assay ID: Hs00702289_s1), and GAPDH mRNA was measured as an endogenous control (assay ID: Hs02758991_g1) (both from Applied Biosystems, Foster City, CA, USA). A high capacity cDNA reverse transcription kit (cat. # 4374966; Applied Biosystems) was used to convert total RNA to single-stranded cDNA for positive control analysis. Reactions contained 2 μl of RT buffer (10X), 0.8 μl of deoxynucleotide triphosphate (25X), 2 μl of random primers (10X), 1 μl of multiscribe RT enzyme (500 U/μl), 1 μl of RNase inhibitor, 3.2 μl of nuclease-free water and 10 μl of extracted total RNA. The reactions were incubated at 25˚C for 10 min, 37˚C for 2 h, and 85˚C for 5 sec (Perkin Elmer 9600 GeneAmp PCR system; Applied Biosystems). Real-time PCR reactions were performed with TaqMan 2X Universal master mix (no AmpErase UNG) (cat. # 4304437; Applied Biosystems) and TaqMan gene expression assays (listed previously). Reactions contained 10 μl of TaqMan Universal PCR master mix (no AmpErase UNG), 1 μl of TaqMan gene expression assay (20X), 2 μl of cDNA template and 7 μl of nuclease-free water.

For miRNA analysis, total RNA from transfections was used to synthesise cDNA using the high-capacity cDNA reverse transcription kit and miRNA-specific RT primers for miR-222 (cat. # 4427975), miR-25 (cat. # 4427975), and endogenous control RNU6B (cat. # 4427975) (Applied Biosystems) in 15 μl reactions. Reactions contained 0.15 μl of 25X dNTP mixture (100 mM), 1 μl of multiScribe reverse transcriptase (50 U/μl), 1.5 μl of reverse transcription buffer (10X), 0.19 μl of RNase inhibitor, 4.16 μl of nuclease-free water, 3 μl of RT primer and 5 μl of extracted total RNA. The reactions were incubated at 16˚C for 30 min, 42˚C for 30 min, 85˚C for 5 min and then an indefinite hold at 4˚C (Perkin Elmer 9600 GeneAmp PCR system; Applied Biosystems). miRNA expression was then assessed using sequence specific primers from the TaqMan microRNA assays and TaqMan 2X Universal master mix (no AmpErase UNG) (cat. # 4304437; Applied Biosystems) in 20 μl reactions according to the manufacturer's instructions. Reactions contained 1 μl of TaqMan miRNA assay mix (20X), 1.33 μl of product from RT reaction (1:15 dilution), 10 μl of TaqMan 2X Universal master mix (no AmpErase UNG) and 7.67 μl of nuclease free water. Each assay was performed in triplicate for each sample.

All real-time PCR reactions were incubated in a 96-well optical plate (cat. # N8010560; Applied Biosystems) at 95˚C for 10 min, following by 40 cycles of 95˚C for 15 sec and 60˚C for 1 min on the Applied Biosystems 7900HT Real-Time PCR system (Applied Biosystems). Study files were generated using a fixed threshold of 0.1 on the SDS2.2.2 software (Applied Biosystems), and Microsoft Excel (Microsoft, Redmond, WA, USA) was used to perform $\Delta\Delta$Ct analysis on the real-time PCR output (18).

RNA isolation and mRNA microarray analysis. Total RNA was isolated from transfected cell lines using PARIS™ Protein

and RNA isolation kit (cat. # AM1556; Ambion) and RNeasy mini kit (cat. # 74104; Qiagen, Venlo, The Netherlands). Briefly, the cells were lysed with PARIS Cell Disruption Buffer and 2X Lysis/Binding Solution. Cell lysates were then transferred to Qiagen QIAshredder columns followed by RNA extraction and on column DNase treatment (Cat. # 79254; Qiagen, Venlo, The Netherlands) according to the manufacturer's instructions. RNA nanogram concentration per microlitre was verified using a NanoDrop spectrophotometer (ND-1000; Labtech International, Lewes, UK) and RNA integrity was verified using a 2100 Bioanalyser (Agilent, Santa Clara, CA, USA).

Affymetrix GeneChip Human Gene 1.0 ST arrays were used for gene expression analysis according to the manufacturer's instructions (cat. # 902461; Affymetrix, Santa Clara, CA, USA). Three biological repeats were used for each treatment. Microarray statistical analysis was performed on .CEL files using the Partek Genomics Suite (Partek Inc., St. Louis, MO, USA; www.partek.com). Data were normalised and summarised using the robust multi-average method, as previously described (19). Paired t-tests were performed to compare the data from the pre-miR transfections to the negative control transfections. Comparisons were corrected for multiple testing using the false discovery rate (FDR). Genes were deemed to be differentially regulated in the pre-miR™ transfected cells if they possessed a FDR ≤0.05 and a fold change ≥2. Gene functional and pathway enrichment analysis was assessed by the PANTHER database (http://www.pantherdb.org/).

Fluidigm reverse transcription-PCR analysis of target genes downregulated by miR-222 and miR-25. Total RNA from transfections was converted to single-stranded cDNA using the High Capacity cDNA Reverse Transcription kit (cat. # 4374966; Applied Biosystems) in 20 μl reactions, as described in the transfection section of this manuscript.

Pre-amplification of cDNA was performed using the TaqMan PreAmp Master Mix kit (cat. # 4384267; Applied Biosystems). The assays used were as follows: MAL2; Hs00294541_m1, MAL; Hs00242748_m1, TLR3; Hs01551078_m1, ADM; Hs00181605_m1, RAB19; Hs01397748_m1, PDCD1LG2; Hs00228839_m1, RAD51; Hs00947968_m1, ADAM21; Hs01652548_s1, HYOU1; Hs01026180_m1, THBS1; Hs00962908_m1, ETS1; Hs00428287_m1, FGFR2; Hs03466165_gH, CYR61; Hs00609994_m1, PHLDB2; Hs01083801_m1, BIRC3; Hs00154109_m1, PRKAA2; Hs00178903_m1, CYP24A1; Hs00989011_g1, AOX1; Hs00154079_m1, MYO5C; Hs00218921_m1, GPR126; Hs01097890_m1, CDK6; Hs00608037_m1, PPME1; Hs00211693_m1, RBM24; Hs00290607_m1, TNFSF10/TRAIL; Hs00921974_m1, ITGA6; Hs01041012_m1, MPP1; Hs00609971_m1, TIMP2; Hs00234278_m1, ITGA3; Hs01076876_m1, ADAMTS1; Hs00199608_m1, ITGA5; Hs00233732_m1, TRIP13; Hs01020073_m1, MAP2K4; Hs00387426_m1, RAB23; Hs00212407_m1, ADAM10; Hs00153853_m1, TRHDE; Hs00183821_m1, RAB14; Hs00249440_m1, RARB; Hs00233405_m1, MAN2A1; Hs00159007_m1, RGS4; Hs00194501_m1, PTGS2; Hs00153133_m1, EPGN; Hs02385425_m1, SNAP23; Hs01047498_m1, LHFPL2; Hs00299613_m1, MYO1B; Hs01031676_m1, NFIA; Hs00906448_m1, RNF38; Hs01014398_m1 (all from Applied Biosystems). Before running the pre-amplification reaction, the intended assays were pooled together, as per the manufacturer's instructions, with 1X Tris-EDTA (TE) buffer in a 0.2X pooled assay mix. The pre-amplification reaction was performed in 5 μl reactions containing 2.5 μl of TaqMan PreAmp master mix (2X), 1.25 μl of the pooled assay mix (0.2X), and 1.25 μl of cDNA sample (100 ng). The pre-amplification reaction was performed for 10 min at 95˚C, and 14 cycles of 15 sec at 95˚C and 4 min at 60˚C (PE 9600 GeneAmp PCR system; Applied Biosystems).

The Fluidigm Dynamic Arrays facilitate the testing of the expression of 48 genes in 48 samples by performing 2,304 PCR assays per chip. The TaqMan gene expression assays listed in the previous paragraph were diluted to a final concentration of 10X using Fluidigm DA Assay Loading Reagent (cat. # 100-7611; Fluidigm, South San Francisco, CA, USA), and the pre-amplified products, diluted to 1:5 using 1X TE buffer. The cDNA product was combined with real-time PCR reagents in 5 μl reactions as follows: 2.25 μl of diluted pre-amplified cDNA, 2.25 μl Universal PCR master mix (2X) (cat. # 4304437; Applied Biosystems), and 0.25 μl Fluidigm sample loading agent (cat. # 100-7610; Fluidigm). Samples, primers and probes were then loaded onto the Fluidigm 48.48 Dynamic Arrays and placed on the IFC controller (both from Fluidigm) which pressure-loads the assay components into the reaction chambers. Assay components are automatically combined on-chip. The Biomark Real-Time PCR system (Fluidigm) was then used for thermal cycling and fluorescence detection. cDNA from transfections was loaded in duplicate on three replicate dynamic arrays. Microsoft Excel (Microsoft) was used to perform ΔΔCt analysis on the real-time PCR output, as previously described (18).

Protein extraction and western blotting. Protein was isolated from transfections using ice-cold radioimmunoprecipitation assay (RIPA) buffer (cat. # R0278; Medical Supply Co., Dublin, Ireland) with added protease and phosphatase inhibitor cocktails (cat. # 04693116001 and 04693116001 respectively; Roche, Indianapolis, IN, USA). Samples were suspended in SDS-PAGE sample buffer (cat. # S3401; Sigma-Aldrich, St. Louis, MO, USA), boiled for 4 min, and resolved on 10% SDS-PAGE gels. The separated proteins were electrophoretically transferred to PVDF membranes by the semi-dry transfer technique for 1 h. PVDF membranes were subsequently blocked in 5% non-fat dried milk in TBS-0.1% Tween-2 (TBS-T) for 1 h at room temperature, washed three times in TBS-T, and incubated with primary antibodies (polyclonal rabbit anti-human mitogen-activated protein kinase kinase 4 (MEK4) (sc-964; Santa Cruz Biotechnology, Inc., Santa Cruz, CA, USA) diluted to 1:50, or monoclonal mouse anti-human TNF-related apoptosis-inducing ligand (TRAIL) (ab12124) at 2 μg/ml, or monoclonal mouse anti-human GAPDH (ab8245) (diluted to 1:25,000) (both from Abcam, Cambridge, UK) overnight at 4˚C with gentle rocking. After three washes in TBS-T, the membranes were incubated with the appropriate HRP-labelled secondary antibodies [goat anti-mouse IgG-HRP, goat anti-rabbit IgG-HRP (cat. # 7076 and 7074 respectively; Cell Signaling Technology, Danvers, MA, USA)] for 1 h at room temperature. The membranes were washed three times in TBS-T and immunoreactive bands were visualised using a HRP development solution containing 100 mM Tris-HCl pH 8.8, 30% H_2O_2, 250 mM luminol, and 90 mM

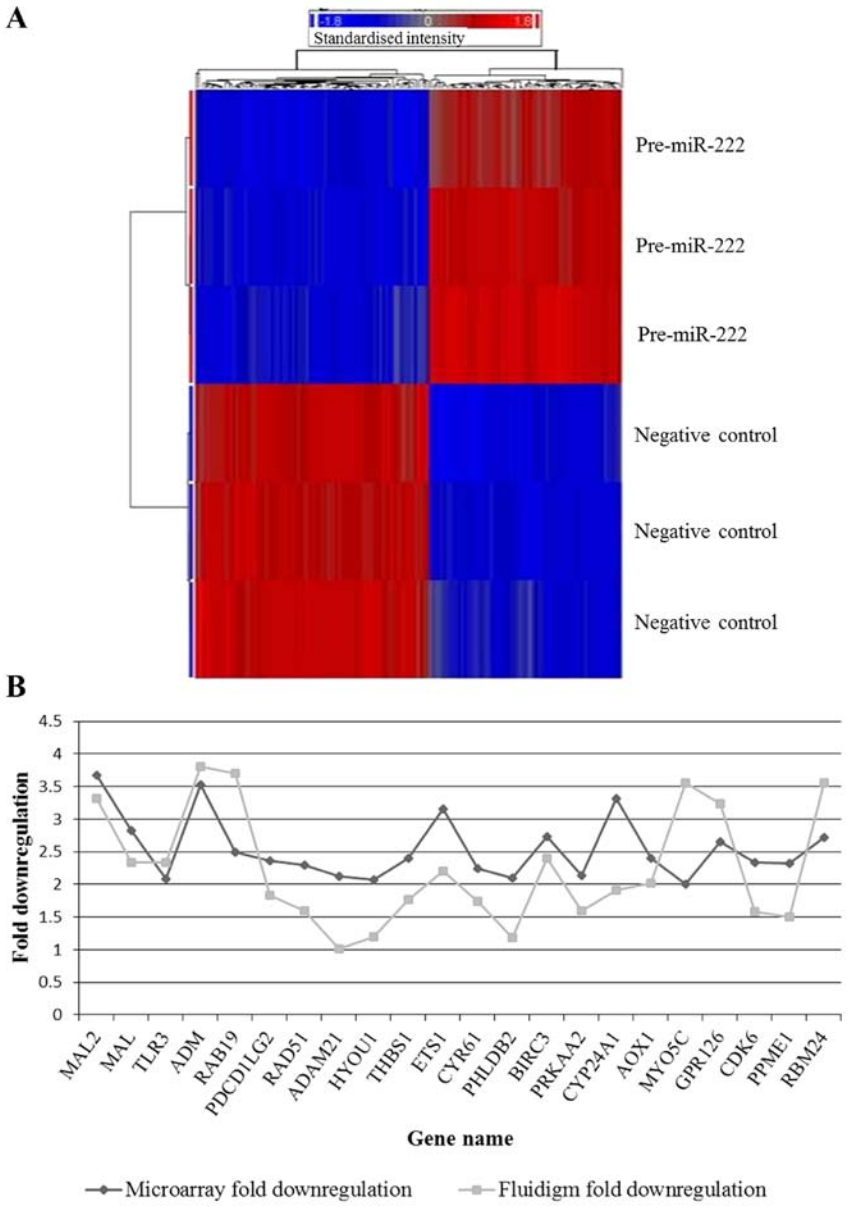

Figure 1. miR-222 regulated genes. (A) Heat map of the significantly differentially regulated genes in pre-miR-222 treated Nthy-ori cells compared to negative control treated cells, false discovery rate (FDR) ≤0.05 and fold-change ≥2. A clear separation can be seen between the genes in pre-miR treated samples compared to negative control treated samples. (B) Line graph of the microarray and Fluidigm fold downregulation of the 22 genes validated by real-time PCR. All genes validated were found to be downregulated by both real-time PCR and microarray analyses (Pearson's correlation, 0.506).

4-iodophenylboronic acid (4-IPBA), and subsequent exposure to Kodak light-sensitive film (cat. # F5763-50EA; Sigma-Aldrich). Jurkat T cell lysates were a gift from Dr Michael Freeley and were used as postive control lysates in western blot experiments

Results

As has been previously noted, expression of miR-222 is upregulated in thyroid cancers compared to their normal counterparts (2-5), while expression of miR-25 is downregulated in anaplastic thyroid carcinoma (5,16). We therefore investigated the impact of overexpression of miR-222 in normal Nthy-ori cells, and of miR-25 in the 8505C cells. An average 2.9-fold upregulation of miR-222 and 10,939-fold upregulation of miR-25 was observed with the pre-miR transfections (n=3). The very large miR-25 fold change increase resulted from an average Ct change of 20.95 in the pre-miR-25 treated cells compared to 33.53 in the cells treated with the negative control pre-miR. Reduced transfection efficiency in the normal Nthy-ori cells may explain the more modest increase in miR-222 post-transfection; however, the positive control gene, *PTK9*, was downregulated to a similar extent in both cell lines; 82.9 and 76.9% in the 8505C and Nthy-ori cells respectively. Microarray analysis elucidated the genes significantly downregulated (FDR value ≤0.05 and fold-change ≥2) by pre-miR-222 in Nthy-ori cells and pre-miR-25 in 8505C cells. We found that overexpression of miR-222 in normal Nthy-ori cells resulted in the downregulation of 82 target genes, while overexpression of miR-25 resulted in the downregulation of 98 target genes in 8505C cells. Figs. 1A and 2A illustrate the genes that were significantly downregulated by pre-miR-222 and pre-miR-25, respectively (see Tables I and II for full gene

Table I. All significantly downregulated genes in pre-miR-222 treated cells compared to cells treated with negative control pre-miRs.

RefSeq	Gene symbol	Gene assignment	Fold change	P-value (FDR)
NM_015913	TXNDC12	Thioredoxin domain containing 12 (endoplasmic reticulum)	-4.807	1.02E-07
NM_000700	ANXA1	Annexin A1	-3.881	2.24E-08
NM_052886	MAL2	Mal, T cell differentiation protein 2	-3.681	1.16E-07
NM_005139	ANXA3	Annexin A3	-3.595	1.48E-09
NM_004493	HSD17B10	Hydroxysteroid (17-beta) dehydrogenase 10	-3.548	3.73E-10
NM_001124	ADM[b]	Adrenomedullin	-3.526	1.08E-09
NM_020373	ANO2	Anoctamin 2	-3.475	1.68E-07
NM_000782	CYP24A1	Cytochrome P450, family 24, subfamily A, polypeptide 1	-3.321	1.71E-06
NM_005238	ETS1[b]	V-ets erythroblastosis virus E26 oncogene homolog 1 (avian)	-3.159	2.16E-08
NM_003494	DYSF	Dysferlin, limb girdle muscular dystrophy 2B (autosomal recessive)	-3.057	8.62E-09
NM_019026	TMCO1	Transmembrane and coiled-coil domains 1	-2.935	4.46E-07
NM_007257	PNMA2	Paraneoplastic antigen MA2	-2.916	4.12E-08
NM_031302	GLT8D2	Glycosyltransferase 8 domain containing 2	-2.853	1.19E-07
NM_002371	MAL	Mal, T cell differentiation protein	-2.830	4.19E-08
NM_001165	BIRC3	Baculoviral IAP repeat-containing 3	-2.734	6.86E-08
NM_153020	RBM24[b]	RNA binding motif protein 24	-2.717	1.34E-05
NM_020651	PELI1	Pellino homolog 1 (*Drosophila*)	-2.668	4.42E-06
NM_020455	GPR126	G protein-coupled receptor 126	-2.659	9.57E-08
NM_004572	PKP2	Plakophilin 2	-2.630	7.81E-10
NM_012431	SEMA3E	Sema domain, immunoglobulin domain (Ig), short basic doma in, secreted, (semaphorin) 3E	-2.625	1.83E-05
NM_002780	PSG4	Pregnancy specific beta-1-glycoprotein 4	-2.606	8.80E-08
NM_002764	PRPS1	Phosphoribosyl pyrophosphate synthetase 1	-2.599	1.99E-08
NM_014322	OPN3	Opsin 3	-2.581	9.04E-07
NM_013322	SNX10	Sorting nexin 10	-2.569	2.18E-07
NM_182757	RNF144B	Ring finger 144B	-2.519	1.61E-09
NM_000716	C4BPB	Complement component 4 binding protein beta	-2.519	6.66E-05
NM_020127	TUFT1	Tuftelin 1	-2.519	3.51E-08
NM_001008749	RAB19	RAB19, member RAS oncogene family	-2.501	8.91E-07
NM_017439	PION	Pigeon homolog (*Drosophila*)	-2.499	3.05E-05
NM_018639	WSB2	WD repeat and SOCS box-containing 2	-2.482	4.86E-08
NM_014143	CD274	CD274 molecule	-2.420	5.96E-07
NM_003246	THBS1	Thrombospondin 1	-2.403	1.78E-08
NM_001159	AOX1	Aldehyde oxidase 1	-2.403	2.50E-06
NM_000141	FGFR2	Fibroblast growth factor receptor 2	-2.394	2.56E-06
NM_003901	SGPL1	Sphingosine-1-phosphate lyase 1	-2.380	1.82E-06
NM_002296	LBR	Lamin B receptor	-2.368	2.36E-08
NM_025239	PDCD1LG2	Programmed cell death 1 ligand 2	-2.360	7.42E-06
NM_004741	NOLC1	Nucleolar and coiled-body phosphoprotein 1	-2.351	6.16E-07
NM_002998	SDC2[a]	Syndecan 2	-2.333	2.69E-07
NM_001259	CDK6[c]	Cyclin-dependent kinase 6	-2.332	2.46E-07
NM_016147	PPME1	Protein phosphatase methylesterase 1	-2.326	1.44E-08
NM_004482	GALNT3	UDP-N-acetyl-alpha-D-galactosamine: polypeptide N-acetylgalactosaminyltransferase 3 (GalNAc-T3)	-2.314	4.48E-06
NM_021069	SORBS2	Sorbin and SH3 domain containing 2	-2.314	2.89E-07
NM_005264	GFRA1	GDNF family receptor alpha 1	-2.304	5.49E-07
NM_022131	CLSTN2	Calsyntenin 2	-2.298	7.38E-08
NM_002875	RAD51	RAD51 homolog (RecA homolog, *E. coli*) (*S. cerevisiae*)	-2.295	2.71E-06
BC066649	C1orf198	Chromosome 1 open reading frame 198	-2.275	2.03E-07

Table I. Continued.

RefSeq	Gene symbol	Gene assignment	Fold change	P-value (FDR)
AK131040	LOC388022	Hypothetical gene supported by AK131040	-2.259	8.18E-05
BC016278	LOH3CR2A	Loss of heterozygosity, 3, chromosomal region 2, gene A	-2.243	0.0004969
NM_001554	CYR61	Cysteine-rich, angiogenic inducer, 61	-2.241	6.15E-07
NM_033393	FHDC1	FH2 domain containing 1	-2.237	3.51E-07
NM_002492	NDUFB5	NADH dehydrogenase (ubiquinone) 1 beta subcomplex, 5	-2.225	1.36E-07
NM_018327	SPTLC3	Serine palmitoyltransferase, long chain base subunit 3	-2.225	6.97E-07
NM_080670	SLC35A4	Solute carrier family 35, member A4	-2.211	6.39E-07
NM_022772	EPS8L2	EPS8-like 2	-2.202	3.77E-08
NM_014391	ANKRD1	Ankyrin repeat domain 1 (cardiac muscle)	-2.191	7.78E-08
NM_016206	VGLL3	Vestigial like 3 (*Drosophila*)	-2.191	8.67E-07
Ensembl no: ENST00000319426	-	Partially transcribed sequence	-2.188	4.57E-06
NM_004694	SLC16A6	Solute carrier family 16, member 6 (monocarboxylic acid transporter 7)	-2.184	0.0003082
NM_021623	PLEKHA2	Pleckstrin homology domain containing, family A (phosphoinositide binding specific) member 2	-2.160	1.74E-06
NR_002836	PGM5P2	Phosphoglucomutase 5 pseudogene 2	-2.159	2.55E-07
NM_001145204	LOC729993	Hypothetical protein LOC729993, transcript variant 1, mRNA	-2.148	2.73E-07
NM_153345	TMEM139	Transmembrane protein 139	-2.143	3.58E-06
NR_002836	PGM5P2	Phosphoglucomutase 5 pseudogene 2	-2.141	4.39E-08
NM_006252	PRKAA2	Protein kinase, AMP-activated, alpha 2 catalytic subunit	-2.137	7.04E-07
NM_002547	OPHN1	Oligophrenin 1	-2.137	2.60E-07
NM_016132	MYEF2	Myelin expression factor 2	-2.136	4.39E-05
NM_003813	ADAM21	ADAM metallopeptidase domain 21	-2.121	0.0005355
Ensembl no: ENST00000384701	-	Expressed sequence tag (EST)	-2.116	0.0002848
NM_145753	PHLDB2	Pleckstrin homology-like domain, family B, member 2	-2.099	4.55E-05
NM_001415	EIF2S3	Eukaryotic translation initiation factor 2, subunit 3 gamma, 52 kDa	-2.096	2.72E-07
NM_000331	SAA1	Serum amyloid A1	-2.086	0.0041182
NM_003265	TLR3	Toll-like receptor 3	-2.082	5.79E-05
NM_006389	HYOU1	Hypoxia up-regulated 1	-2.077	1.02E-07
NM_015238	WWC1	WW and C2 domain containing 1	-2.069	1.56E-07
NM_001001522	TAGLN	Transgelin	-2.056	9.60E-07
Ensembl no: ENST00000322446	-	Partially transcribed sequence	-2.042	0.0007311
NM_006832	FERMT2	Fermitin family homolog 2 (*Drosophila*)	-2.005	3.07E-05
NM_018728	MYO5C	Myosin VC	-2.003	9.51E-07
NM_002354	EPCAM	Epithelial cell adhesion molecule	-2.018	0.0224988

[a]Predicted target in miRanda, PicTar and TargetScan; [b]predicted target in PicTar and TargetScan; [c]predicted target in TargetScan.

lists). The PANTHER database was used to perform gene ontology analysis on these pre-miR target lists. This analysis illustrated that the two miRNAs target genes of diverse functions in the thyroid cells, as no pathway was significantly over- or under-represented in either list. This observation concurs with other studies on miRNA target prediction and elucidation (20-22). miR-222 and miR-25 target lists were also cross-referenced with *in silico* prediction results from three prediction algorithms: miRanda, PicTar and TargetScan.

Overexpression of miR-222 in Nthy-ori cells. Five of the 82 genes (6.1%) significantly downregulated by miR-222 overexpression in the Nthy-ori 3-1 cells were predicted gene targets of the miRNA in miRanda, PicTar or TargetScan, or a combination of the databases. Gene ontology analysis revealed that no molecular function or biological process was significantly over- or underrepresented in the miR-222 target list. Notwithstanding this observation, several genes that were found to be targets of this miRNA have interesting

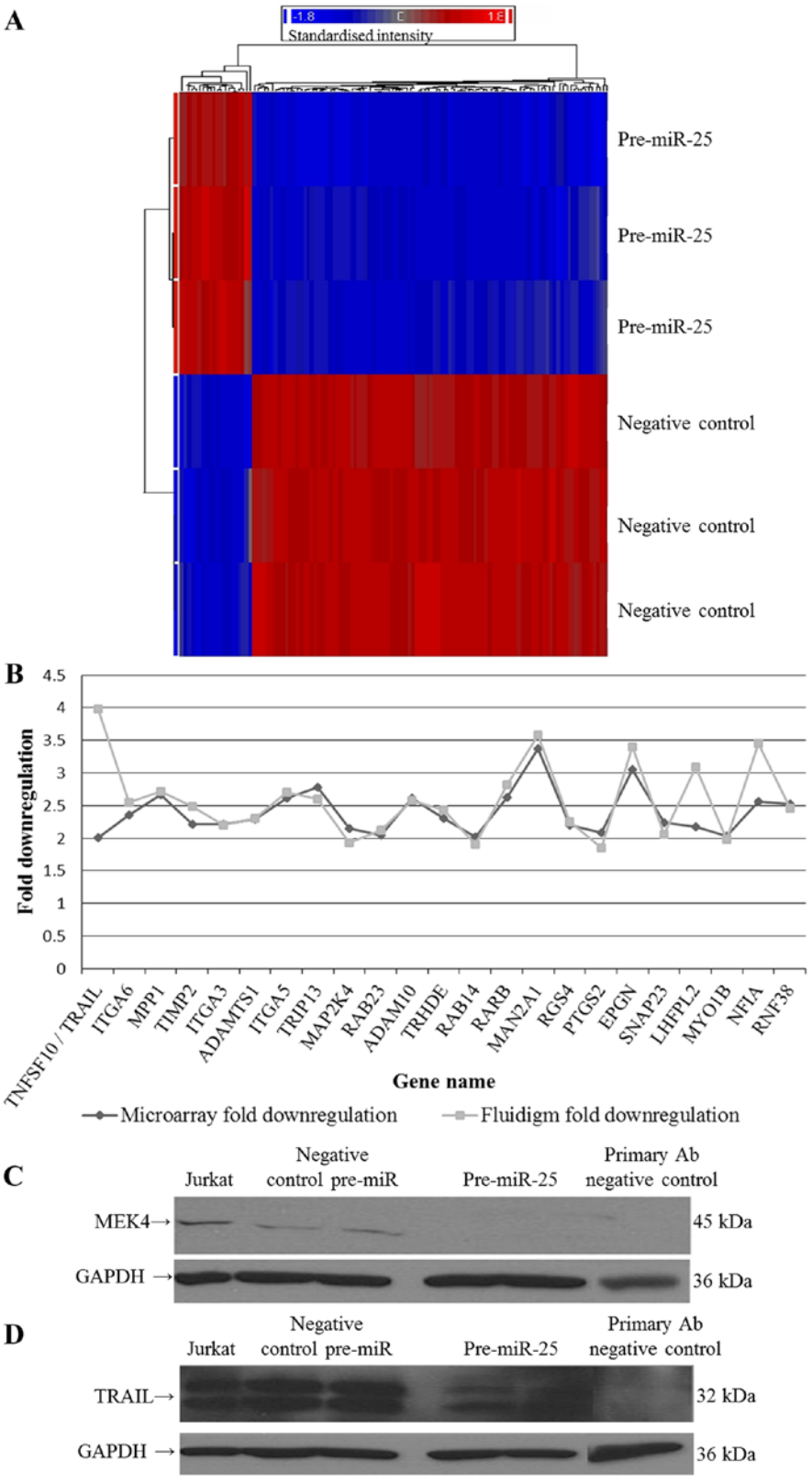

Figure 2. miR-25 regulated genes. (A) Heat map of the significantly differentially regulated genes in pre-miR-25 treated 8505C cells compared to negative control treated cells; false discovery rate (FDR) ≤0.05 and fold-change ≥2. A clear separation can be seen between the genes in pre-miR treated samples compared to negative control treated samples. (B) Line graph of the microarray and Fluidigm fold downregulation of the 23 genes validated by real-time PCR. All genes validated were found to be downregulated by both real-time PCR and microarray analyses [Pearson's correlation, 0.538, TNF-related apoptosis-inducing ligand (TRAIL) removed, 0.810]. (C) Western blotting results for mitogen-activated protein kinase kinase 4 (MEK4) expression in 8505C cells. Jurkat T cell lysate acts as a positive control for expression of MEK4. There are two lanes where protein from negative control and pre-miR-25 transfected cells was loaded, and untreated 8505C protein was loaded and acted as a 'no primary antibody' negative control as it was only exposed to secondary antibody. GAPDH acts as a loading control. A band of the correct size for MEK4 (45 kDa) was detected on the blot. The reduction of MEK4 in the pre-miR-25 treated cells successfully validates the fact that pre-miR-25 decreases the expression of this protein. (D) Western blotting results for TRAIL expression in 8505C cells. Lane titles are the same as the previous blot. Bands of approximately the correct size for TRAIL (32 kDa) were detected in the cell lysates tested. The reduction of TRAIL in the pre-miR-25 treated cells successfully validates the fact that pre-miR-25 decreases the expression of this protein.

Table II. All significantly downregulated genes in pre-miR-25 treated cells compared to cells treated with negative control pre-miRs.

RefSeq	Gene symbol	Gene assignment	Fold change	P-value (FDR)
NM_000210	ITGA6	Integrin alpha 6	-2.352	6.17E-09
NM_002372	MAN2A1[b]	Mannosidase, alpha, class 2A, member 1	-3.370	4.98E-10
NM_002436	MPP1	Membrane protein, palmitoylated 1	-2.669	1.08E-09
NM_003255	TIMP2	TIMP metallopeptidase inhibitor 2	-2.218	1.75E-09
NM_021913	AXL[d]	AXL receptor tyrosine kinase	-2.594	2.49E-09
NM_015881	DKK3	Dickkopf homolog 3 (*Xenopus laevis*)	-3.428	2.89E-09
NM_018442	IQWD1[c]	IQ motif and WD repeats 1	-2.134	2.97E-09
NM_002204	ITGA3	Integrin alpha 3 (antigen CD49C, alpha 3 subunit of VLA-3 receptor)	-2.209	7.00E-09
NM_004035	ACOX1	Acyl-Coenzyme A oxidase 1, palmitoyl	-2.206	1.42E-08
NM_005562	LAMC2	Laminin gamma 2	-2.803	1.12E-08
NM_006520	DYNLT3[d]	Dynein, light chain, Tctex-type 3	-2.694	1.07E-08
NM_006988	ADAMTS1	ADAM metallopeptidase with thrombospondin type 1 motif 1	-2.285	1.34E-08
NM_006080	SEMA3A[e]	Sema domain, immunoglobulin domain (Ig), short basic domain, secreted, (semaphorin) 3A	-2.450	2.61E-08
NM_000351	STS	Steroid sulfatase (microsomal), isozyme S	-2.410	2.36E-08
NM_019004	ANKIB1	Ankyrin repeat and IBR domain containing 1	-2.304	1.15E-08
NM_181659	NCOA3	Nuclear receptor coactivator 3	-2.006	1.41E-08
NM_002844	PTPRK	Protein tyrosine phosphatase receptor type K	-2.152	1.97E-08
NM_002205	ITGA5[a]	Integrin alpha 5 (fibronectin receptor, alpha polypeptide)	-2.614	9.07E-09
NM_000916	OXTR	Oxytocin receptor	-2.473	4.16E-08
NM_005349	RBPJ	Recombination signal binding protein for immunoglobulin kappa J region	-2.033	4.83E-08
NM_005471	GNPDA1	Glucosamine-6-phosphate deaminase 1	-2.236	1.42E-08
NM_004237	TRIP13	Thyroid hormone receptor interactor 13	-2.781	1.02E-08
NM_001418	EIF4G2[e]	Eukaryotic translation initiation factor 4 gamma, 2	-2.494	1.95E-08
NM_021999	ITM2B	Integral membrane protein 2B	-2.070	3.95E-08
NM_000138	FBN1[b]	Fibrillin 1	-2.355	2.18E-07
NM_003010	MAP2K4[b]	Mitogen-activated protein kinase kinase 4	-2.147	1.34E-08
NM_016275	SELT	Selenoprotein T	-3.175	2.35E-08
NM_001102445	RGS4	Regulator of G-protein signaling 4	-2.194	3.62E-08
NM_001001521	UGP2[b]	UDP-glucose pyrophosphorylase 2	-3.032	6.61E-08
NM_002948	RPL15	Ribosomal protein L15	-2.659	4.97E-08
NM_003139	SRPR[b]	Signal recognition particle receptor ('docking protein')	-2.195	1.33E-07
NM_001190	BCAT2[b]	Branched chain aminotransferase 2, mitochondrial	-3.040	7.52E-08
NM_000693	ALDH1A3	Aldehyde dehydrogenase 1 family, member A3	-2.168	2.58E-06
NM_012242	DKK1	Dickkopf homolog 1 (*Xenopus laevis*)	-2.060	3.20E-07
NM_006178	NSF	N-ethylmaleimide-sensitive factor	-2.202	4.09E-07
NM_199511	CCDC80	Coiled-coil domain containing 80	-2.016	1.25E-07
NM_014674	EDEM1[b]	ER degradation enhancer, mannosidase alpha-like 1	-2.391	8.84E-08
NM_213611	SLC25A3	Solute carrier family 25 (mitochondrial carrier; phosphate carrier)	-2.086	1.17E-07
NM_133494	NEK7	NIMA (never in mitosis gene a)-related kinase 7	-2.424	3.00E-07
NM_017958	PLEKHB2	Pleckstrin homology domain containing, family B2 (evectins) member	-3.420	8.84E-08
NM_000259	MYO5A	Myosin VA (heavy chain 12, myoxin)	-2.426	2.11E-07
NM_016277	RAB23[b]	RAB23, member RAS oncogene family	-2.051	1.26E-07
NM_001110	ADAM10[b]	ADAM metallopeptidase domain 10	-2.616	3.21E-07
NM_001693	ATP6V1B2	ATPase, H^+ transporting, lysosomal 56/58 kDa, V1 subunit B2	-2.064	1.30E-07
NM_005779	LHFPL2[a]	Lipoma HMGIC fusion partner-like 2	-2.173	1.72E-07
NM_016422	RNF141[e]	Ring finger protein 141	-2.260	8.57E-08
NM_002095	GTF2E2	General transcription factor IIE, polypeptide 2, beta 34k	-2.570	7.22E-07
NM_003483	HMGA2[e]	High mobility group AT-hook 2	-2.654	1.24E-07
NM_014223	NFYC[c]	Nuclear transcription factor Y, gamma	-2.112	1.57E-07
NM_013381	TRHDE	Thyrotropin-releasing hormone degrading enzyme	-2.306	2.96E-07
NM_006287	TFPI	Tissue factor pathway inhibitor (lipoprotein-associated coagulation inhibitor)	-2.145	5.36E-07
NM_033540	MFN1	Mitofusin 1	-2.014	3.46E-07

Table II. Continued.

RefSeq	Gene symbol	Gene assignment	Fold change	P-value (FDR)
NM_024664	PPCS[b]	Phosphopantothenoylcysteine synthetase	-2.386	3.87E-07
NM_023080	C8orf33	Chromosome 8 open reading frame 33	-2.006	1.98E-07
NM_016352	CPA4	Carboxypeptidase A4	-2.060	1.26E-06
NM_012223	MYO1B[b]	Myosin IB	-2.030	1.35E-06
NM_020223	FAM20C	Family with sequence similarity 20 member C	-2.387	1.16E-06
NM_004670	PAPSS2	3'-phosphoadenosine 5'-phosphosulfate synthase 2	-2.347	9.66E-07
NM_005896	IDH1	Isocitrate dehydrogenase 1 ($NADP^+$), soluble	-2.599	3.89E-06
NM_016322	RAB14[b]	RAB14, member RAS oncogene family	-2.021	4.30E-07
NM_002971	SATB1	SATB homeobox 1	-2.080	1.43E-06
NM_000405	GM2A	GM2 ganglioside activator	-2.249	4.07E-07
NM_001547	IFIT2	Interferon-induced protein with tetratricopeptide repeats	-4.287	8.87E-07
NM_016570	ERGIC2	ERGIC and golgi 2	-2.858	9.73E-07
NM_005595	NFIA[b]	Nuclear factor I/A	-2.567	6.45E-07
NM_005981	TSPAN31	Tetraspanin 31	-2.127	6.55E-07
NM_001085471	FOXN3	Forkhead box N3	-2.314	1.11E-06
BC016048	LRRC38	Leucine rich repeat containing 38	-2.394	5.78E-07
NM_005314	GRPR	Gastrin-releasing peptide receptor	-2.545	6.82E-06
NM_002783	PSG7	Pregnancy specific beta-1-glycoprotein 7	-2.015	3.89E-06
NM_002781	PSG5	Pregnancy specific beta-1-glycoprotein 5	-2.222	4.73E-06
NM_003884	KAT2B	K(lysine) acetyltransferase 2B	-2.108	4.43E-06
NM_001040409	MTHFD2	Methylenetetrahydrofolate dehydrogenase ($NADP^+$ dependent) 2, methenyltetrahydrofolate cyclohydrolase	-2.312	1.92E-05
NM_003580	NSMAF[b]	Neutral sphingomyelinase (N-SMase) activation associated factor	-2.072	2.33E-06
NM_001013442	EPGN	Epithelial mitogen homolog (mouse)	-3.057	1.89E-06
NM_012319	SLC39A6	Solute carrier family 39 (zinc transporter), member 6	-2.026	2.95E-06
NM_000965	RARB	Retinoic acid receptor, beta	-2.624	5.42E-06
NM_152772	TCP11L2	T-complex 11 (mouse)-like 2	-2.105	4.63E-05
BC017297	FAM49B	Family with sequence similarity 49 member B	-2.051	1.87E-06
NM_001002265	MARCH8	Membrane-associated ring finger (C3HC4) 8	-2.232	7.22E-06
NM_015509	NECAP1[b]	NECAP endocytosis associated 1	-2.013	1.85E-06
NM_001080512	BICC1	Bicaudal C homolog 1 (*Drosophila*)	-2.193	9.59E-06
NM_001031850	PSG6	Pregnancy specific beta-1-glycoprotein 6	-2.806	7.76E-06
NM_020841	OSBPL8	Oxysterol binding protein-like 8	-2.135	8.37E-06
NM_007036	ESM1	Endothelial cell-specific molecule 1	-2.059	5.81E-06
NM_016075	VPS36	Vacuolar protein sorting 36 homolog (*S. cerevisiae*)	-2.021	3.55E-06
NM_000963	PTGS2	Prostaglandin-endoperoxide synthase 2 (prostaglandin G/H synthase and cyclooxygenase)	-2.084	9.13E-06
NM_017946	FKBP14	FK506 binding protein 14, 22 kDa	-2.240	1.13E-05
NM_003825	SNAP23	Synaptosomal-associated protein, 23 kDa	-2.233	6.08E-06
NM_194328	RNF38[a]	Ring finger protein 38	-2.526	7.91E-06
NM_006636	MTHFD2	Methylenetetrahydrofolate dehydrogenase ($NADP^+$ dependent) 2, methenyltetrahydrofolate cyclohydrolase	-2.362	0.0001745
NM_006905	PSG1	Pregnancy specific β-1-glycoprotein 1	-2.016	0.0001079
Ensembl no: ENST00000390952	-	Expressed Sequence Tag (EST)	-2.078	0.0001661
NM_030920	ANP32E[e]	Acidic (leucine-rich) nuclear phosphoprotein 32 family, member E	-2.663	6.01E-05
NM_000262	NAGA	N-acetylgalactosaminidase, alpha	-2.055	4.77E-05
NM_001548	IFIT1	Interferon-induced protein with tetratricopeptide repeats	-2.439	3.00E-05
NM_001039569	AP1S3	Adaptor-related protein complex 1, sigma 3 subunit	-2.193	0.0003395
NM_003810	TNFSF10	Tumour necrosis factor (ligand) superfamily, member 10	-2.003	0.0011012

[a]Predicted target in miRanda, PicTar and TargetScan; [b]predicted target in PicTar and TargetScan; [c]predicted target in miRanda and TargetScan; [d]predicted target in miRanda; [e]predicted target in TargetScan.

Table III. Downregulated genes following expression of pre-miR-222 in Nthy-ori 3-1.

Gene	Microarray fold downregulation	Microarray P-value (FDR)	Fluidigm qPCR fold downregulation	Fluidigm P-value (t-test)
MAL2	3.681	1.16E-07	3.314	3.55E-05
MAL	2.83	4.19E-08	2.332	1.54E-05
TLR3	2.082	5.79E-05	2.341	0.0001
ADM[a]	3.526	1.08E-09	3.81	2.93E-05
RAB19	2.501	8.91E-07	3.7	4.48E-06
PDCD1LG2	2.36	7.42E-06	1.827	0.004
RAD51	2.295	2.71E-06	1.597	9.59E-05
ADAM21	2.121	0.0005	1.008	0.9517
HYOU1	2.077	1.02E-07	1.198	0.0001
THBS1	2.403	1.78E-08	1.769	0.0002
ETS1[a]	3.159	2.16E-08	2.208	0.0003
CYR61	2.241	6.15E-07	1.745	0.0006
PHLDB2	2.099	4.55E-05	1.178	0.003
BIRC3	2.734	6.86E-08	2.406	0.0005
PRKAA2	2.137	7.04E-07	1.595	0.001
CYP24A1	3.321	1.71E-06	1.911	0.0006
AOX1	2.403	2.50E-06	2.024	0.0006
MYO5C	2.003	9.51E-07	3.549	0.0002
GPR126	2.659	9.57E-08	3.24	6.8E-05
CDK6[b]	2.332	2.46E-07	1.588	0.0004
PPME1	2.326	1.44E-08	1.5	0.0006
RBM24[a]	2.717	1.34E-05	3.55	3.11E-06

[a]Predicted target in PicTar and TargetScan; [b]predicted target in TargetScan.

molecular functions. For instance, seven receptors are in the lists (*MAL*, *OPN3*, *PSG4*, *FGFR2*, *GPR126*, *TLR3* and *LBR*), four transcription factors (*PSG4*, *ETS1*, *MAL* and *RBM24*), five signalling molecules (*THBS1*, *ETS1*, *CYR61*, *SEMA3E* and *ADM*), and five genes involved in defence and immunity (*PNMA2*, *C4BPB*, *SDC2*, *MAL*, *TLR3* and *SAA1*).

The downregulation of 22 genes in response to miR-222 overexpression identified by the microarray analysis (both predicted and novel targets) was successfully validated using Fluidigm real-time PCR technologies (Table III and Fig. 1B) (Pearson's correlation, 0.506).

Overexpression of miR-25 in 8505C cells. The list of 98 miR-25 target genes was also cross-referenced with *in silico* prediction results. This comparison revealed that the list of genes that were significantly downregulated by pre-miR-25 in the 8505C cells is enriched with 27/98 or 27.55% predicted gene targets for miR-25. Gene ontology analysis of the miR-25 gene target list suggests that cell adhesion is an important aspect of miR-25 functioning in the thyroid cells as biological processes including cell adhesion, cell communication, signal transduction, and cell adhesion-mediated signalling were significantly enriched for in this list (P-value 1.47E-02, 1.18E-03, 3.13E-02 and 1.59E-02, respectively). The list is also significantly enriched for cell adhesion molecules: *ITGA3*, *ITGA5* (which is also a predicted target of the miRNA in all three databases used); and *ITGA6* (P-value 3.10E-03) and CAM family adhesion molecules: *PSG1*, *PSG5*, *PSG6* and *PSG7* (P-value 2.47E-02). Seven receptors are also in the miR-25 list: *TCP11L2*, *RARB*, *GRPR*, *PTPRK*, *AXL*, *LRRC38* and *OXTR*; six transcription factors: *RARB*, *FOXN3*, *SATB1*, *NCOA3*, *GTF2E2* and *NFIA*; and five kinases: *MPP1*, *AXL*, *MAP2K4*, *PAPSS2* and *NEK7*, and a member of the tumour necrosis family, *TNFSF10/TRAIL*.

Fluidigm real-time PCR technologies were used to confirm the downregulation of 23 predicted and novel gene targets in response to miR-25 expression in the 8505C cells (Table IV and Fig. 2B). All genes tested were downregulated in both the microarray and Fluidigm analyses (Pearson's correlation, 0.538; *TRAIL* removed, 0.810). In addition, two novel targets of miR-25 were successfully validated at the protein level by western blotting; predicted target MEK4 and novel target TRAIL. Fig. 2C and D illustrate the reduction in MEK4 and TRAIL protein expression following treatment of anaplastic thyroid cells with pre-miR-25, demonstrating that they are direct or indirect targets of this miRNA.

Discussion

The aim of this study was to elucidate the mRNA targets of two miRNAs that we had previously found to be differentially expressed in thyroid cancer (5): miR-222 and miR-25. This was achieved by overexpressing the thyroid cancer-associated miRNA miR-222 in the transformed normal Nthy-ori cells, and miR-25 in the anaplastic cancer-derived 8505C cells.

Table IV. Downregulated genes following expression of pre-miR-25 in 8505C cells.

Gene	Microarray fold downregulation	Microarray P-value (FDR)	Fluidigm qPCR fold downregulation	Fluidigm P-value (t-test)
TNFSF10/TRAIL	2.003	0.001	3.982	0.003
ITGA6	2.352	6.17E-09	2.552	0.0002
MPP1	2.669	1.08E-09	2.718	7.3E-06
TIMP2	2.218	1.75E-09	2.483	2.19E-05
ITGA3	2.209	7.00E-09	2.194	2.40E-07
ADAMTS1	2.285	1.34E-08	2.304	0.002
ITGA5[b]	2.614	9.07E-09	2.699	4.68E-07
TRIP13	2.781	1.02E-08	2.606	4.92E-06
MAP2K4[a]	2.147	1.34E-08	1.925	7.70E-05
RAB23[a]	2.051	1.26E-07	2.122	8.45E-05
ADAM10[a]	2.616	3.21E-07	2.571	1.57E-05
TRHDE	2.306	2.96E-07	2.43	2.09E-06
RAB14[a]	2.021	4.30E-07	1.907	2.91E-05
RARB	2.624	5.42E-06	2.816	7.68E-06
MAN2A1[a]	3.37	4.98E-10	3.576	2.19E-07
RGS4	2.194	3.62E-08	2.255	0.0009
PTGS2	2.084	9.13E-06	1.853	0.0098
EPGN	3.057	1.89E-06	3.394	0.0003
SNAP23	2.233	6.08E-06	2.057	8.58E-05
LHFPL2[b]	2.173	1.72E-07	3.092	0.0002
MYO1B[a]	2.03	1.35E-06	1.986	1.997E-06
NFIA[a]	2.567	6.45E-07	3.445	0.015

[a]Predicted target in PicTar and TargetScan; [b]predicted target in miRanda, PicTar and TargetScan.

The use of microarrays to analyse the RNA from these cells exploited an unbiased genome-wide approach and yielded the discovery of a set of mRNAs that are either directly or indirectly targeted by each miRNA in thyroid cells, and have not been previously described.

The gene target lists produced by this genome-wide investigation compare favourably with previously published studies on miRNA target elucidation and prediction. Similar to prior studies (21,23), the two pre-miRs used in this body of study each downregulated almost 100 target transcripts: 98 by pre-miR-25 in the 8505C cells and 82 by pre-miR-222 in the Nthy-ori 3-1 cells. The subtle change in gene expression observed in the genes targeted by pre-miR-222 and pre-miR-25 (between 2- and 4-fold) is also similar to other studies on the subject (6,21). Finally, the relatively low number of predicted miRNA targets significantly differentially expressed has been noted previously (6), and the divergent assortment of molecular functions and biological processes encompassed within the gene target lists is also reflective of published accounts of target prediction and elucidation (20,21). These diverse lists allow us insight into the functions of these two miRNAs within the respective thyroid cell lines. For instance, upregulation of miR-222 in Nthy-ori cells impacts on several transcription factors, cell signalling molecules, and genes involved in defence and immunity (*PNMA2*, *C4BPB*, *SDC2*, *MAL*, *TLR3* and *SAA1*).

Expression of miR-25 is downregulated in anaplastic thyroid carcinoma, so we upregulated the expression of miR-25 in the anaplastic thyroid carcinoma 8505C cell line. Although miR-25 was found to target genes with a wide variety of functions, the gene ontology analysis of this list highlights the predilection of this miRNA for regulating genes involved in cell adhesion, with both this cellular process and molecules of this molecular function being significantly over-represented in this list. Two main groups of cell adhesion molecules are over-represented in the miR-25 target list; integrin α genes *ITGA3*, *ITGA5* (which is a predicted target of the miR-25 in miRanda, PicTar and TargetScan) and *ITGA6*, and the pregnancy-specific glycoproteins (PSGs); *PSG1*, *PSG5*, *PSG6* and *PSG7*. Loss of miR-25 expression in anaplastic thyroid carcinoma is therefore associated with upregulation of genes encoding integrins and glycoproteins. The *ITGA* genes appear to be markers of aggression in the cancers in which they have been explored. For instance, *ITGA3* and *ITGA5* have been shown to be markers of invasiveness in head and neck squamous cell carcinoma (24), ITGA3, along with ITGB4 and 5 were found to be candidate biomarkers for cervical lymph node metastasis or death in tongue squamous cell carcinoma (25) and ITGA6 was found to be necessary for the tumourigenicity of a stem cell-like subpopulation within the MCF7 breast cancer cell line (26).

This is not the first occasion miR-25 has been linked to a role in cell adhesion, as Xu *et al* have previously highlighted the role of miR-25 in oesophageal squamous cell carcinoma (ESCC). They found upregulation of this miRNA in ESCC cells promoted migration and invasion, and also found that miR-25 directly targets E-Cadherin, an important cellular adhesion protein in the ESCC cells (13). Gerson *et al* have recently identified miR-25, and indeed miR-222, to be responsive to β4 integrin expression in breast carcinoma cell lines (27). Our observation, along with these previous studies in breast cancer and ESCC, indicates a role for miR-25 in tumour progression through the disruption of cell adhesion.

Additional functions of miR-25 are highlighted with the two proteins (MEK4 and TRAIL) that were shown to be downregulated in response to the expression of miR-25. MEK4 is a member of the MAP kinase kinase family that directly phosphorylates and activates c-Jun NH2-terminal kinase (JNK) in response to cellular stresses and pro-inflammatory cytokines, and can also activate p38 (28). MAP kinase signalling is often disrupted in thyroid cancer through *RAS*, *BRAF* or *RET/PTC* mutations (29). Both tumour suppressor and oncogenic functions have been attributed to MEK4 in cancer (30,31). Little is known of the role of MEK4 in thyroid cancer; however, Chiariello *et al* demonstrated that Ret signalling involves MEK4 (32). It remains unclear as to whether MEK4 expression influences anaplastic thyroid carcinoma in a tumour suppressive or oncogenic manner. However, as pre-miR-25 was shown to downregulate MEK4 mRNA and protein in ATC 8505C cells in this study, it is interesting to speculate that the endogenous downregulation of miR-25 may lead to the upregulation of MEK4 expression and its pro-oncogenic characteristics in ATC cells.

TRAIL expression was also decreased in response to miR-25 expression in 8505C cells. TRAIL has five cellular receptors and can activate the extrinsic and intrinsic pathways to regulate intercellular apoptotic responses in the immune system (33). Approximately a decade and a half ago it was noted that TRAIL could induce apoptosis in transformed and malignant cells but not in normal cells (34). TRAIL was subsequently found to be capable of triggering apoptosis in eight PTC and two ATC derived thyroid carcinoma cell lines but not in normal thyrocytes (35). As a result of this tumour-specific effect, a great deal of work was done to develop anticancer therapies to mimic the effect of TRAIL. The TRAIL and MAP kinase pathways appear to overlap in TRAIL therapy signalling. Ohtsuka *et al* reported that the combination of anti-death receptor antibodies and chemotherapy agents led to a synergistic activation of the JNK/p38 MAP kinase which was mediated by MEK4 in breast, prostate and colon cancer cells (36). Moreover, Söderström *et al* showed that MAP/extracellular regulated kinase (ERK) signalling (which is frequently over-activated in thyroid cancer) protected activated T cells from TRAIL-induced apoptosis (37).

miR-25 involvement in the TRAIL-mediated apoptosis pathway was confirmed further with the observation by Razumilava *et al* that this miRNA targets TRAIL death receptor-4 (DR4) and promotes apoptosis resistance in cholangiocarcinoma (38). If one considers the pro-apoptotic role of TRAIL, it is difficult to elucidate how an upregulation of this gene through the endogenous downregulation of miR-25 would be beneficial to the progress of anaplastic thyroid carcinoma. However, a review by Newsom-Davis *et al* outlines *in vitro* and *in vivo* experiments in which TRAIL expression induced proliferation, migration and invasion of tumour cells which were resistant to TRAIL-mediated apoptosis. They describe how secondary intracellular signalling complexes, following TRAIL DISC formation, can activate NF-κB via the inhibitor of κB kinase complex (IKK complex) which signals through MAPK, JNK and p38 (39). Other groups have shown that TRAIL-induced survival and proliferation does not involve the p38 kinase pathway but is dependent on the MAP kinase ERKs. Therefore, in the anaplastic thyroid cancer cells, the endogenous downregulation of miR-25 may enable the upregulation of TRAIL to activate its pro-survival MAP kinase responses (perhaps involving MEK4). Future studies may also benefit from investigating whether miR-25 is involved in regulating MEK4 and TRAIL in response to TRAIL cancer therapies.

In conclusion, this study used an unbiased approach to elucidate almost 100 genes that are either directly or indirectly targeted by miR-25 and miR-222 in thyroid cells. The number of genes in these target lists, the extent to which the genes are regulated and the diversity of their functions is reflective of other published accounts of miRNA target prediction and elucidation. The gene targets of these two miRNAs confirm the diverse nature of miRNA-target interactions within cells. A considerable proportion of these targets have been validated using RT-PCR with a further two, MEK4 and TRAIL, being confirmed at the protein level. We provide an interesting insight into the functions of these two miRNAs in thyroid cells, in particular that cell adhesion and apoptosis are important aspects of miR-25 functioning in thyroid cells. In addition to this, there is broad scope for further investigation of the many results produced by this study.

Acknowledgements

The authors would like to acknowledge grants from the Health Research Board Molecular Medicine PhD training programme and the Science Foundation Ireland funded Molecular Therapeutics for Cancer Ireland.

References

1. Smallridge RC, Marlow LA and Copland JA: Anaplastic thyroid cancer: molecular pathogenesis and emerging therapies. Endocr Relat Cancer 16: 17-44, 2009.
2. He H, Jazdzewski K, Li W, Liyanarachchi S, Nagy R, Volinia S, Calin GA, Liu CG, Franssila K, Suster S, *et al*: The role of microRNA genes in papillary thyroid carcinoma. Proc Natl Acad Sci USA 102: 19075-19080, 2005.
3. Pallante P, Visone R, Ferracin M, Ferraro A, Berlingieri MT, Troncone G, Chiappetta G, Liu CG, Santoro M, Negrini M, *et al*: MicroRNA deregulation in human thyroid papillary carcinomas. Endocr Relat Cancer 13: 497-508, 2006.
4. Nikiforova MN, Tseng GC, Steward D, Diorio D and Nikiforov YE: MicroRNA expression profiling of thyroid tumors: biological significance and diagnostic utility. J Clin Endocrinol Metab 93: 1600-1608, 2008.
5. Aherne ST, Smyth PC, Flavin RJ, Russell SM, Denning KM, Li JH, Guenther SM, O'Leary JJ and Sheils OM: Geographical mapping of a multifocal thyroid tumour using genetic alteration analysis and miRNA profiling. Mol Cancer 7: 89, 2008.
6. Kim HJ, Kim YH, Lee DS, Chung J-K and Kim S: In vivo imaging of functional targeting of miR-221 in papillary thyroid carcinoma. J Nucl Med 49: 1686-1693, 2008.

7. Mitomo S, Maesawa C, Ogasawara S, Iwaya T, Shibazaki M, Yashima-Abo A, Kotani K, Oikawa H, Sakurai E, Izutsu N, *et al*: Downregulation of miR-138 is associated with overexpression of human telomerase reverse transcriptase protein in human anaplastic thyroid carcinoma cell lines. Cancer Sci 99: 280-286, 2008.
8. Keutgen XM, Filicori F, Crowley MJ, Wang Y, Scognamiglio T, Hoda R, Buitrago D, Cooper D, Zeiger MA, Zarnegar R, *et al*: A panel of four miRNAs accurately differentiates malignant from benign indeterminate thyroid lesions on fine needle aspiration. Clin Cancer Res 18: 2032-2038, 2012.
9. Chou CK, Yang KD, Chou FF, Huang CC, Lan YW, Lee YF, Kang HY and Liu RT: Prognostic implications of miR-146b expression and its functional role in papillary thyroid carcinoma. J Clin Endocrinol Metab 98: E196-E205, 2013.
10. Visone R, Russo L, Pallante P, De Martino I, Ferraro A, Leone V, Borbone E, Petrocca F, Alder H, Croce CM and Fusco A: MicroRNAs (miR)-221 and miR-222, both overexpressed in human thyroid papillary carcinomas, regulate $p27^{Kip1}$ protein levels and cell cycle. Endocr Relat Cancer 14: 791-798, 2007.
11. Petrocca F, Vecchione A and Croce CM: Emerging role of miR-106b-25/miR-17-92 clusters in the control of transforming growth factor beta signaling. Cancer Res 68: 8191-8194, 2008.
12. Kim Y-K, Yu J, Han TS, Park SY, Namkoong B, Kim DH, Hur K, Yoo MW, Lee HJ, Yang HK and Kim VN: Functional links between clustered microRNAs: Suppression of cell-cycle inhibitors by microRNA clusters in gastric cancer. Nucleic Acids Res 37: 1672-1681, 2009.
13. Xu X, Chen Z, Zhao X, Wang J, Ding D, Wang Z, Tan F, Tan X, Zhou F, Sun J, *et al*: MicroRNA-25 promotes cell migration and invasion in esophageal squamous cell carcinoma. Biochem Biophys Res Commun 421: 640-645, 2012.
14. Zhang H, Zuo Z, Lu X, Wang L, Wang H and Zhu Z: MiR-25 regulates apoptosis by targeting Bim in human ovarian cancer. Oncol Rep 27: 594-598, 2012.
15. Kan T, Sato F, Ito T, Matsumura N, David S, Cheng Y, Agarwal R, Paun BC, Jin Z, Olaru AV, *et al*: The miR-106b-25 polycistron, activated by genomic amplification, functions as an oncogene by suppressing p21 and Bim. Gastroenterology 136: 1689-1700, 2009.
16. Visone R, Pallante P, Vecchione A, Cirombella R, Ferracin M, Ferraro A, Volinia S, Coluzzi S, Leone V, Borbone E, *et al*: Specific microRNAs are downregulated in human thyroid anaplastic carcinomas. Oncogene 26: 7590-7595, 2007.
17. Esposito F, Tornincasa M, Pallante P, Federico A, Borbone E, Pierantoni GM and Fusco A: Down-regulation of the miR-25 and miR-30d contributes to the development of anaplastic thyroid carcinoma targeting the polycomb protein EZH2. J Clin Endocrinol Metab 97: E710-E718, 2012.
18. Livak KJ and Schmittgen TD: Analysis of relative gene expression data using real-time quantitative PCR and the 2(-Delta Delta C(T)) Method. Methods 25: 402-408, 2001.
19. Irizarry RA, Hobbs B, Collin F, Beazer-Barclay YD, Antonellis KJ, Scherf U and Speed TP: Exploration, normalization, and summaries of high density oligonucleotide array probe level data. Biostatistics 4: 249-264, 2003.
20. Lewis BP, Shih IH, Jones-Rhoades MW, Bartel DP and Burge CB: Prediction of mammalian microRNA targets. Cell 115: 787-798, 2003.
21. Lim LP, Lau NC, Garrett-Engele P, Grimson A, Schelter JM, Castle J, Bartel DP, Linsley PS and Johnson JM: Microarray analysis shows that some microRNAs downregulate large numbers of target mRNAs. Nature 433: 769-773, 2005.
22. Bartel DP: MicroRNAs: target recognition and regulatory functions. Cell 136: 215-233, 2009.
23. Brennecke J, Stark A, Russell RB and Cohen SM: Principles of microRNA-target recognition. PLoS Biol 3: e85, 2005.
24. Yu YH, Kuo HK and Chang KW: The evolving transcriptome of head and neck squamous cell carcinoma: a systematic review. PLoS One 3: e3215, 2008.
25. Kurokawa A, Nagata M, Kitamura N, Noman AA, Ohnishi M, Ohyama T, Kobayashi T, Shingaki S and Takagi R; Oral, Maxillofacial Pathology, and Surgery Group: Diagnostic value of integrin alpha3, beta4, and beta5 gene expression levels for the clinical outcome of tongue squamous cell carcinoma. Cancer 112: 1272-1281, 2008.
26. Cariati M, Naderi A, Brown JP, Smalley MJ, Pinder SE, Caldas C and Purushotham AD: Alpha-6 integrin is necessary for the tumourigenicity of a stem cell-like subpopulation within the MCF7 breast cancer cell line. Int J Cancer 122: 298-304, 2008.
27. Gerson KD, Maddula VSRK, Seligmann BE, Shearstone JR, Khan A and Mercurio AM: Effects of β4 integrin expression on microRNA patterns in breast cancer. Biol Open 1: 658-666, 2012.
28. Cuenda A: Mitogen-activated protein kinase kinase 4 (MKK4). Int J Biochem Cell Biol 32: 581-587, 2000.
29. Fagin JA and Mitsiades N: Molecular pathology of thyroid cancer: diagnostic and clinical implications. Best Pract Res Clin Endocrinol Metab 22: 955-969, 2008.
30. Wang L, Pan Y and Dai JL: Evidence of MKK4 pro-oncogenic activity in breast and pancreatic tumors. Oncogene 23: 5978-5985, 2004.
31. Xin W, Yun KJ, Ricci F, Zahurak M, Qiu W, Su GH, Yeo CJ, Hruban RH, Kern SE and Iacobuzio-Donahue CA: MAP2K4/MKK4 expression in pancreatic cancer: genetic validation of immunohistochemistry and relationship to disease course. Clin Cancer Res 10: 8516-8520, 2004.
32. Chiariello M, Visconti R, Carlomagno F, Melillo RM, Bucci C, de Franciscis V, Fox GM, Jing S, Coso OA, Gutkind JS, *et al*: Signalling of the Ret receptor tyrosine kinase through the c-Jun NH2-terminal protein kinases (JNKS): evidence for a divergence of the ERKs and JNKs pathways induced by Ret. Oncogene 16: 2435-2445, 1998.
33. Mahalingam D, Szegezdi E, Keane M, de Jong S and Samali A: TRAIL receptor signalling and modulation: are we on the right TRAIL? Cancer Treat Rev 35: 280-288, 2009.
34. Ashkenazi A and Dixit VM: Apoptosis control by death and decoy receptors. Curr Opin Cell Biol 11: 255-260, 1999.
35. Mitsiades N, Poulaki V, Tseleni-Balafouta S, Koutras DA and Stamenkovic I: Thyroid carcinoma cells are resistant to FAS-mediated apoptosis but sensitive to tumor necrosis factor-related apoptosis-inducing ligand. Cancer Res 60: 4122-4129, 2000.
36. Ohtsuka T, Buchsbaum D, Oliver P, Makhija S, Kimberly R and Zhou T: Synergistic induction of tumor cell apoptosis by death receptor antibody and chemotherapy agent through JNK/p38 and mitochondrial death pathway. Oncogene 22: 2034-2044, 2003.
37. Söderström TS, Poukkula M, Holmström TH, Heiskanen KM and Eriksson JE: Mitogen-activated protein kinase/extracellular signal-regulated kinase signaling in activated T cells abrogates TRAIL-induced apoptosis upstream of the mitochondrial amplification loop and caspase-8. J Immunol 169: 2851-2860, 2002.
38. Razumilava N, Bronk SF, Smoot RL, Fingas CD, Werneburg NW, Roberts LR and Mott JL: miR-25 targets TNF-related apoptosis inducing ligand (TRAIL) death receptor-4 and promotes apoptosis resistance in cholangiocarcinoma. Hepatology 55: 465-475, 2012.
39. Newsom-Davis T, Prieske S and Walczak H: Is TRAIL the holy grail of cancer therapy? Apoptosis 14: 607-623, 2009.